

# Surface Fitting of Rapidly Varying Data Using Rank Coding: Application to Geophysical Surfaces<sup>1</sup>

Christian Gout<sup>2</sup> and Dimitri Komatitsch<sup>3</sup>

---

*Addressing geophysical problems often implies the correct description of surfaces with large local variations. This problem is of interest in many areas of geophysics—for instance, for the description of topography when studying site effects in seismic wave propagation, or the propagation of lava or pyroclastic flows along the slopes of a volcano, or in the presence of geological structures with faults. However, surface fitting of rapidly varying data using classical functions like splines is known to be difficult. Without information about the location of the large variations in the data set, the usual approximation methods lead to instability phenomena or undesirable oscillations. We propose a new approach that uses scale transformations, and whose originality consists in a preprocessing and a postprocessing of the data. Variations of the unknown function are reduced using a scale transformation in the preprocessing phase. The transformed data do not exhibit large variations, and therefore we can use a usual approximant that will not create oscillations. An inverse scale transformation is subsequently applied. We discuss the convergence of the method when the number of data points tends to infinity. We show the efficiency of this technique by applying it to a Digital Elevation Model of the topography of the Piton de la Fournaise volcano (Réunion Island, France).*

---

**KEY WORDS:** splines; scale transformation; surfaces; topography; rank coding.

## INTRODUCTION

In many problems of geophysical interest, when trying to describe surfaces, one has to deal with data that exhibit rapid local variations. This occurs, for instance, when describing the topography of mountain ranges, volcanoes, islands, or the shape of geological entities, which can exhibit large and rapid variations due to the presence of faults in the structure. The correct description of such geological surfaces, by a fitting process from a given set of points, is therefore of great importance (Mallet, 1992). This is particularly true when one needs to describe topographic models with good regularity, usually  $C^0$  or  $C^1$ , from the knowledge of a given low- or

---

<sup>1</sup>Received 30 March 1999; accepted 7 December 1999.

<sup>2</sup>Department of Applied Mathematics, ERS 2055-CNRS, Université de Pau, France. e-mail: christian.gout@univ-pau.fr

<sup>3</sup>Department of Earth and Planetary Sciences, Harvard University, Cambridge, Massachusetts 02138, USA. e-mail: komatits@seismology.harvard.edu

medium-resolution set of surface points, often called a digital elevation model (DEM). This is typically the case, for instance, when studying site effects and ground motion amplification related to topography in seismic wave propagation problems and earthquake hazard assessment (Frankel and Leith, 1992; Bouchon, Schultz, and Töksoz, 1996; Komatitsch and Vilotte, 1998; Komatitsch and others, 1999), or when studying the propagation of pyroclastic flows or lava flows along the slopes of a volcano (Ishihara, Iguchi, and Kamo, 1990).

Unfortunately, when applied to the approximation of surfaces from rapidly varying data, usual methods like splines lead to strong oscillations near steep gradients, as illustrated in Figure 1. When the location of the large variations in the dataset is known, Salkauskas (1974) and Foley (1987) have proposed methods that use a spline under tension with a nonconstant smoothing parameter, and Hsieh and Chang (1994) have proposed a concept of virtual nodes inserted at the level of the large variations in the case of an approximant in the context of computer-aided geometric design. In the more general context when the location of the large variations in the dataset is not known *a priori*, Franke (1985) and Bouhamidi (1992) have proposed splines under tension belonging to more general spaces. These methods give good results in the case of curve fitting, but less accurate results in the case of surface fitting. Other approaches such as the Discrete Smooth Interpolation have also been used successfully to address the problem (Mallet, 1992, 1997).

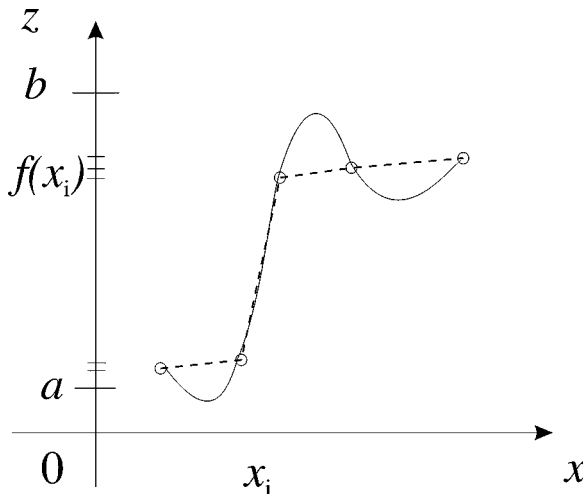


**Figure 1.** When classical splines (for instance, here a  $C^1$  spline, solid line) are used to interpolate data points  $(x_i, f(x_i))$  with large local variations (dashed line), strong spurious oscillations are generated near steep gradients.

The new method we introduce here uses scale transformations, and is applied without any particular *a priori* knowledge of the data. The philosophy of the method is similar to interpolation methods based upon anamorphosed data commonly used in geostatistics (see, for instance, Issaks and Srivastava, 1989). In the first part of this article, a construction of the scale transformation families is presented. Results concerning the convergence of the approximation are given without proof. In the second part, we show the efficiency of this innovative approach by applying it to the topography of the summit of the Piton de la Fournaise volcano, located in the Réunion Island (Indian Ocean, France). This volcano exhibits large and rapid variations in steep river valleys in its southwestern part, as well as in a caldera, where the behavior of the method is tested.

### DESCRIPTION OF THE METHOD

The method we propose uses two scale transformations—namely  $\varphi_d$  for the preprocessing and  $\psi_d$  for the postprocessing. The first one,  $\varphi_d$ , is used to transform the  $z$  values representing the height of the unknown surface  $f$  into values  $(u_i)$ , regularly distributed in an interval chosen by the user, as illustrated in Figures 2A and 2B. The preprocessing function  $\varphi_d$  is such that the transformed data do not exhibit large local variations, and therefore a usual spline operator  $T^d$  can subsequently be applied without generating significant oscillations, as shown in Figure 2C. The second scale transformation  $\psi_d$  is then applied to the approximated values to map them back and obtain the approximated values of  $z$  (Fig. 2D). It is important to underline that the proposed scale transformations do not create spurious oscillations. Moreover, this method is applied without any particular knowledge of the location of the large variations in the dataset.

Let us consider a dataset  $(x_i^d, z_i^d)_{i=1, \dots, N(d)}^d$  indexed with a real  $d$ , such that when  $d$  tends to 0, the number of data points  $N(d)$  tends to infinity. For the purpose of a theoretical study of the convergence of the approximation, we introduce a function  $f : \Omega \rightarrow [a, b]$ , such that the data set becomes  $(x_i^d, z_i^d = f(x_i^d))_{i=1, \dots, N(d)}^d$ . The functions introduced above have the following expression, for  $m \in \mathbb{N}$  :

$$\begin{aligned} &-\varphi_d: [a, b] \rightarrow [\alpha, \beta] \subset \mathbb{R}, \\ &-T^d: (\varphi_d \circ f) \in H^m(\Omega, [\alpha, \beta]) \rightarrow T^d(\varphi_d \circ f) \in H^m(\Omega, [\alpha, \beta]), \\ &-\psi_d \circ (T^d(\varphi_d \circ f)) \in H^m(\Omega, [a, b]), \end{aligned}$$

where the preprocessing  $\varphi_d$  and the postprocessing  $\psi_d$  are continuous scale transformations families, where  $T^d$  is an approximation operator, for instance a spline, and where  $H^m(\Omega, \cdot)$  denotes the usual Sobolev space. More precisely, we introduce a bounded nonempty connected set  $\Omega$  with a Lipschitz-continuous boundary of  $\mathbb{R}^2$ , and an unknown function  $f \in H^{m'}(\Omega, [a, b])$  that we want to approximate, this hypothesis allowing to have  $(\varphi_d \circ f)$  bounded in  $C^m(\bar{\Omega})$  (with  $m' > m + 1$ ),

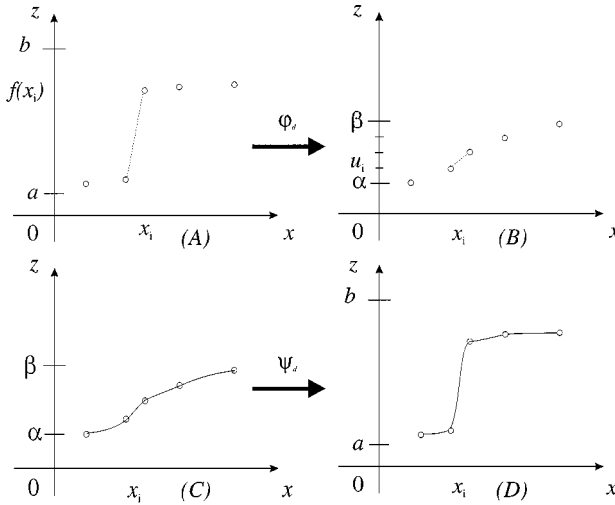


**Figure 2.** The preprocessing phase, A and B, transforms the values  $f(x_i)$  using a scale transformation  $\varphi_d$ . After preprocessing, B, the local variations in the data have been drastically reduced. Therefore, it is possible to obtain a regular approximant with no significant oscillations using an usual  $C^1$  spline operator, as shown in C. A second scale transformation  $\psi_d$  is subsequently applied to the values of the approximant in a postprocessing phase, D, to map them back and obtain the final approximant. It is important to mention that the scale transformations used do not create spurious oscillations, as illustrated in D.

a property used to establish the convergence of the approximation (Gout, 1999). We also consider a subset  $A^d$  of  $N = N(d)$  distinct points of  $\bar{\Omega}$  such that

$$\sup_{x \in \bar{\Omega}} \delta(x, A^d) = d \tag{1}$$

where  $\delta$  is the Euclidean distance of  $\mathbb{R}^2$ ; the index  $d$  represents the radius of the biggest sphere included in  $\Omega$  that does not intersect with any point of  $A^d$ , and thus, when  $d$  tends to 0, the number of data points tends to infinity. We also introduce the set  $Z_1^d$  of  $N = N(d)$  real numbers such that

$$\forall x_i^d \in A^d, \quad f(x_i^d) \in Z_1^d \tag{2}$$

and the sequence  $Z_2^d$  of  $p(d)$  distinct  $z$  values obtained from the ordering of  $Z_1^d$ ,  $\forall z_i^d \in Z_2^d, i = 1, \dots, p(d)$ ,

$$a = \tilde{z}_1^d < \tilde{z}_2^d < \tilde{z}_3^d < \dots < \tilde{z}_{p(d)-1}^d < \tilde{z}_{p(d)}^d = b \tag{3}$$

where  $[a, b] = \text{Im}(f)$ . The sequence  $Z_2^d$  will be used for the construction of the scale transformation families in the following section. In what follows, for convenience, we also write  $(z_i)$  instead of  $(z_i^d)$ .

### Scale Transformation Families

In this section, we give a construction of the scale transformation families by generalizing the technique introduced by Apprato (1987) and Torrens (1991). These scale transformations are realistic in the sense that, as classical transformations, they are monotonous.

#### *Preprocessing of the Data: Family $(\varphi_d)$ of Scale Transformations*

The goal of the scale transformation  $\varphi_d$  is to reduce the variations in the data set. We first construct  $\varphi_d$ , and in order to study the convergence of the approximation, we then establish the convergence of  $\varphi_d$  to a function  $\varphi$  when the number of data points tends to infinity (i.e.,  $d \rightarrow 0$ ). Let  $[\alpha, \beta]$  be an interval of  $\mathbb{R}$ , and  $\{u_i\}_{i=1, \dots, p(d)}$ , the following regular subdivision, for  $i = 1, \dots, p(d)$ ,

$$\alpha = u_1 < u_2 < u_3 < \dots < u_{p(d)-1} < u_{p(d)} = \beta \quad \text{and} \quad u_{i+1} - u_i = \frac{\beta - \alpha}{p(d) - 1} \quad (4)$$

These interval and subdivision are chosen by the user. When dealing with surface approximation from rapidly varying data, we choose the interval to be  $[0, 1]$ , and an even subdivision of the  $\{u_i\}$  that is used to reduce the local variations of the  $(z_i)$ . After applying  $\varphi_d$ , we obtain a new data set  $(x_i, u_i)$  related to the initial data by  $u_i = \varphi_d(z_i)$ . When this technique is applied to other problems, however, for instance in some applications in imaging, when one has an image with homogeneous grey levels, it can on the contrary be of interest to increase the variations between pixels values—the  $(z_i)$ —; in such a case, Gout (1997) showed that it is possible to choose a nonregular distribution in the interval  $[\alpha, \beta]$  to generate variations, and therefore to enhance some features present in the image to facilitate its segmentation.

We introduce  $\varphi : [a, b] \rightarrow [\alpha, \beta]$  the  $C^\infty$  diffeomorphism that transforms  $[a, b]$  into  $[\alpha, \beta]$  (such families of transformations are usually called anamorphosis in the geostatistics literature):

$$\varphi(z) = \frac{\beta - \alpha}{b - a}(z - a) + \alpha \quad (5)$$

We also introduce the function  $\varphi_d$ , for  $i = 1, \dots, p(d) - 1$ , and for any

$z \in [z_i, z_{i+1}]$ ,

$$\begin{aligned} \varphi_d(z) &= u_i q_{0m}^0 \left( \frac{z - z_i}{z_{i+1} - z_i} \right) + u_{i+1} q_{0m}^1 \left( \frac{z - z_i}{z_{i+1} - z_i} \right) \\ &\quad + \alpha_1(z_i)(z_{i+1} - z_i) q_{1m}^0 \left( \frac{z - z_i}{z_{i+1} - z_i} \right) \\ &\quad + \alpha_1(z_{i+1})(z_{i+1} - z_i) q_{1m}^1 \left( \frac{z - z_i}{z_{i+1} - z_i} \right) \end{aligned} \tag{6}$$

where the  $q_{lm}^i$ , for  $i = (0, 1)$ , and  $l = (0, 1)$ , are the basis functions of the finite element of class  $C^m$  on  $[0, 1]$  (Ciarlet, 1978) and where, for any  $i = 1, \dots, p(d) - 1$ ,

$$\alpha_1(z_i) = \frac{u_{i+1} - u_i}{z_{i+1} - z_i} \quad \text{and} \quad \alpha_1(z_{p(d)}) = \alpha_1(z_{p(d)-1}) \tag{7}$$

Using relations (3)–(6), we obtain the following results:  $\varphi_d$  implements the interpolation of the  $(u_i)$ , and  $\varphi_d$  belongs to  $C^m[a, b]$  :

- (i)  $\varphi_d(z_i) = u_i$ , for  $i = 1, \dots, p(d)$ ;
- (ii)  $\varphi_d \in C^m[a, b]$ .

We now consider a *sufficient* convergence hypothesis, which implies that the distribution of the data  $(z_i)$  has an asymptotic regularity in the interval  $[a, b]$  when  $d$  tends to 0, and which is used to establish the convergence of the approximation. This hypothesis is that there exists  $C > 0$  and  $m'' \in \mathbb{N}$  verifying  $m'' \geq m \geq 2$  such that, for  $d$  small enough, and for any  $i = 1, \dots, p(d) - 2$ , we have

$$\left| 1 - \frac{z_{i+1} - z_i}{z_{i+2} - z_{i+1}} \right| \leq C \left( \frac{b - a}{p(d) - 1} \right)^{m''} \tag{8}$$

We also suppose that the set  $A^d$  introduced above satisfies that there exists  $C' > 0$  such that

$$p(d) \leq \frac{C'}{d^2} \tag{9}$$

Equation (9), introduced by Arcangéli (1986), expresses a property of asymptotic regularity of the distribution of the data set  $A^d$  in  $\bar{\Omega}$ . Using a compactness argument, Gout (1998) established that hypotheses (8) and (9) imply that there exists  $C'' > 0$ , such that  $\|\varphi_d\|_{C^m[a,b]} \leq C''$  and

$$\lim_{d \rightarrow 0} \varphi_d = \varphi \text{ in } C^0([a, b]) \tag{10}$$

where  $\varphi_d$  is defined by (6), and  $\varphi$  is defined by (5).

One can notice that construction of the scale transformations  $\varphi_d$  made in (6) uses a finite difference scheme of order 1 to construct, from the  $u_i$ , the first derivatives of  $\varphi_d$  at the points  $\tilde{z}_i, i = 1, \dots, p(d)$ . Moreover, the option retained in (6), which is to cancel the  $l$  derivatives of  $\varphi_d$  at the points  $\tilde{z}_i$  for any  $l = 2, \dots, m$ , could be substituted by the option consisting in using a finite difference scheme of order  $l$  to define these  $l$  derivatives. Let us also mention that we have chosen to construct scale transformations on a finite element basis in order to be able to study convergence of the approximation.

*Postprocessing of the Data: Family ( $\psi_d$ ) of Scale Transformations*

Similar to the way we constructed the scale transformations  $\varphi_d$ , we now define a scale transformation family  $\psi_d$  that implements the postprocessing of the calculation. We recall that after the preprocessing, the large local variations in the data set have been drastically reduced; therefore it is possible to approximate the data using a usual spline operator  $T^d$  without generating significant oscillations. To map these values back and obtain the approximated values of  $z$ , we need to use a postprocessing step, and therefore need to introduce a family ( $\psi_d$ ), which is almost the inverse of ( $\varphi_d$ ): as  $\varphi_d$  converges to  $\varphi$ , we construct  $\psi_d$  such that  $\psi_d$  converges to  $\varphi^{-1}$ . To do so, we define the  $C^\infty$  diffeomorphism  $\varphi^{-1} : [\alpha, \beta] \rightarrow [a, b]$  inverse of  $\varphi$  defined in Equation (5):

$$\varphi^{-1}(u) = \frac{(u - \alpha)(b - a)}{\beta - \alpha} + a \tag{11}$$

We also define  $\psi_d$  the function, for  $i = 1, \dots, p(d) - 1$ , and for any  $u \in [u_i, u_{i+1}]$ ,

$$\begin{aligned} \psi_d(u) = & z_i q_{0m}^0 \left( \frac{u - u_i}{u_{i+1} - u_i} \right) + z_{i+1} q_{0m}^1 \left( \frac{u - u_i}{u_{i+1} - u_i} \right) \\ & + (u_{i+1} - u_i) \beta_1(u_i) q_{1m}^0 \left( \frac{u - u_i}{u_{i+1} - u_i} \right) \\ & + (u_{i+1} - u_i) \beta_1(u_{i+1}) q_{1m}^1 \left( \frac{u - u_i}{u_{i+1} - u_i} \right) \end{aligned} \tag{12}$$

where the  $q_{lm}^i$ , for  $i = (0, 1)$ , and  $l = (0, 1)$  are the basis functions of the finite element of class  $C^m$  on  $[0, 1]$  and where

$$\beta_1(u_i) = \frac{z_{i+1} - z_i}{u_{i+1} - u_i} \quad \text{and} \quad \beta_1(u_{p(d)}) = \beta_1(u_{p(d)-1}) \tag{13}$$

Under hypotheses (8) and (9), Gout (1998) established the following relations:

- (i)  $\psi_d(u_i) = z_i, \quad i = 1, \dots, p(d);$
- (ii)  $\psi_d \in C^m[\alpha, \beta];$
- (iii) there exists  $C > 0,$  such that  $\|\psi_d\|_{C^m[\alpha, \beta]} \leq C$
- (iv)  $\lim_{d \rightarrow 0} \psi_d = \varphi^{-1}$  in  $C^0([\alpha, \beta]).$

It is important to mention that (i) is one of the key points of the algorithm, that (ii) allows us to obtain approximants with high regularity, and that (iii) and (iv) are used to establish the convergence of the approximation.

### The Smoothing Spline Operator

Given a Lagrange dataset  $(x_i, (\varphi_d \circ f)(x_i) = \varphi_d(z_i))$ , we have to solve the classical problem of constructing an approximant  $T^d$  of class  $C^k$  (with  $k = 1$  or  $2$  in practice). In this work, we use a smoothing  $D^m$  spline, as defined in Arcangéli (1986) and Arcangéli (1989), which has many advantages: it is possible to implement a local refinement, the matrix of the linear system to solve is banded, and it is possible to study convergence of the approximation. We have chosen to use a smoothing  $D^m$  spline and not an interpolation spline because we want to be able to work with large data sets of up to several hundreds of thousands of points, and in that case, a smoothing spline is far less expensive than an interpolation spline.

We consider the functional, for any  $\Phi \in H^m(\Omega),$

$$J_\varepsilon^d(\Phi) = \langle \rho^d(\Phi - \varphi_d \circ f) \rangle_d^2 + \varepsilon |\Phi|_{m,\Omega}^2 \tag{14}$$

where  $\rho^d \in L(H^m(\Omega), \mathbb{R}^{p(d)})$  is defined by  $\rho^d f = (f(a))_{a \in A^d} \in \mathbb{R}^{p(d)}, |\cdot|_{m,\Omega}$  is the usual seminorm of  $H^m(\Omega), \langle \cdot \rangle_d$  is the usual norm in  $\mathbb{R}^{p(d)},$  and  $\varepsilon$  is a smoothing parameter. We call  $\sigma_\varepsilon^d$  the  $D^m$ -smoothing spline on  $\Omega$  relative to  $\rho^d(\varphi_d \circ f),$  which is the unique solution of the minimization problem: for any  $\Phi \in H^m(\Omega),$  find  $\sigma_\varepsilon^d \in H^m(\Omega)$  such that

$$J_\varepsilon^d(\sigma_\varepsilon^d) \leq J_\varepsilon^d(\Phi) \tag{15}$$

The solution  $\sigma_\varepsilon^d$  to this problem is also the unique solution of the variational problem: for any  $\Phi \in H^m(\Omega),$  find  $\sigma_\varepsilon^d \in H^m(\Omega)$  such that

$$\langle \rho^d \sigma_\varepsilon^d, \rho^d \Phi \rangle_d + \varepsilon (\sigma_\varepsilon^d, \Phi)_{m,\Omega} = \langle \rho^d(\varphi_d \circ f), \rho^d \Phi \rangle_d \tag{16}$$

Uniqueness of the solution can be proved using the Lax–Milgram lemma and results by Necas (1967) to establish the equivalence of norms.

In order to compute  $\sigma_\varepsilon^d$ , we choose to discretize it on a finite element basis, which enables us to obtain a small sparse linear system. We choose the generic Bogner–Fox–Schmit (BFS) rectangular finite element (Ciarlet, 1978). In what follows, we use either the BFS of class  $C^0$  or of class  $C^1$  in order to obtain a  $C^0$  or  $C^1$  approximant. In the following, we write  $\sigma_\varepsilon^d$  instead of  $T^d$ .

### Convergence of the Approximation

We first give the convergence of the  $D^m$  spline operator  $\sigma_\varepsilon^d$  related to the transformed data  $(\varphi_d \circ f)$  to the function  $\varphi \circ f$  when  $d$  tends to 0. We obtain this result using the convergence of  $\varphi_d$  to  $\varphi$ , using the fact that Arcangéli (1989) showed that, for any function  $g$ , we have  $\lim_{d \rightarrow 0} \sigma_\varepsilon^d(g) = g$ . Keeping the notation of the previous sections, and since  $(\varphi_d \circ f)$  is bounded in  $C^m(\bar{\Omega})$ , Gout (1998) proved that

$$\lim_{d \rightarrow 0} (\sigma_\varepsilon^d (\varphi_d \circ f)) = \varphi \circ f \text{ in } C^0(\bar{\Omega}). \quad (17)$$

From this result, using a compactness argument, Gout (1999) established a theoretical result concerning the convergence of the approximation:

$$\lim_{d \rightarrow 0} (\psi_d \circ \sigma_\varepsilon^d (\varphi_d \circ f)) = \varphi^{-1} \circ \varphi \circ f = f \text{ in } H^{m-\theta}(\Omega) \quad (18)$$

for any  $\theta > 0$  such that  $\theta < m - 1$  ( $\Rightarrow H^{m-\theta}(\Omega) \hookrightarrow C^0(\bar{\Omega})$ ). Note that if we take  $n = 2$  and  $m = 3$ , the convergence takes place in  $H^{2-\theta}$  for any  $\theta \in ]0, 1[$ .

### APPLICATION TO A VOLCANO

The Piton de la Fournaise is a volcano located in the Indian Ocean, in the Réunion Island, France. This volcano exhibits strong topographic variations near its summit, due to the presence of a caldera and of two steep river valleys in its southwestern part, as can be seen on the picture of the volcano presented in Figure 3. The maximum height of the volcano is 2.6 km, and the depth of the valleys reaches more than 1000 m in several places.

Being able to describe the topography of such regions exhibiting rapid local variations with at least  $C^0$  regularity, or even  $C^1$  regularity, is important in many fields in geophysics. For example, this description of the topography can be an input to numerical modeling codes that study the propagation of pyroclastic flows or lava flows, and related hazards; other examples are seismic site effects and ground motion amplification due to topographic features. In both cases, to avoid creating numerical artefacts, it is important not to introduce spurious oscillations

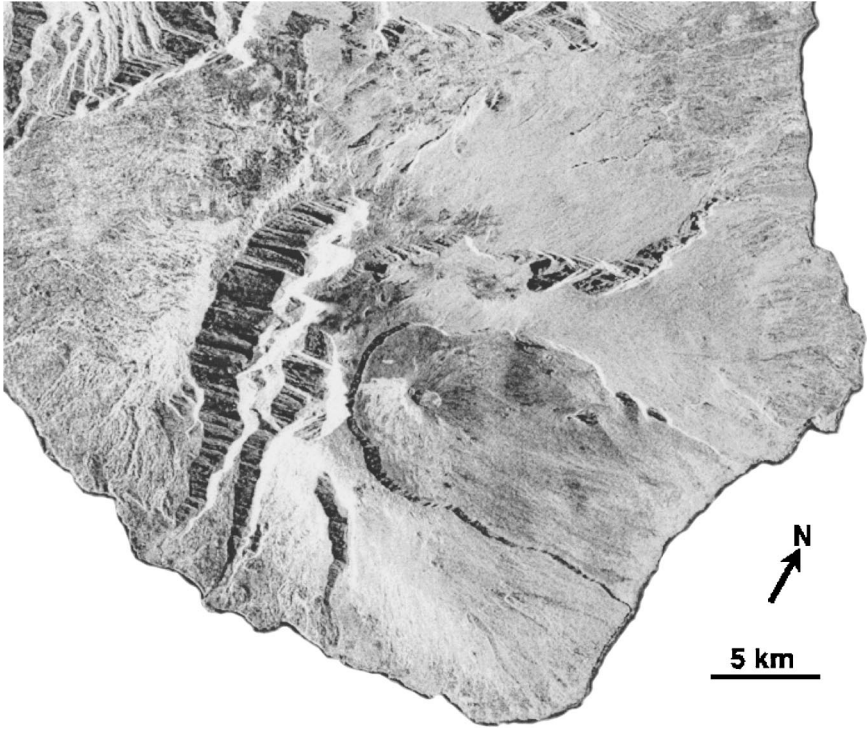


**Figure 3.** Image of the Piton de la Fournaise volcano in the Réunion Island, Indian Ocean, France. One can clearly see the summital caldera, and the two steep valleys in the South–West. The size of the region represented is approximately  $40 \times 35$  km. The height of the volcano is 2.6 km. Image taken as part of the Space Shuttle SIR-C/X-SAR radar missions, courtesy of Pete Mougins-Mark, University of Hawaii.

in the description of the model itself. Otherwise, Komatitsch and Vilotte (1998) and Komatitsch and others (1999) underlined in the context of curvilinear spectral-element modeling of elastic wave propagation that artificial diffraction points appear at the edges between elements, which significantly affects the behavior of surface waves.

To demonstrate the efficiency of our method, we create  $C^0$  and  $C^1$  approximants from a set of 8208 data points taken from a DEM of the summit. The data points in the DEM have been obtained by digitizing a map of the area. In this DEM, the height is given on an evenly spaced grid of  $76 \times 108$  points, with a grid spacing of 200 m. Therefore the region considered has a dimension of 15 km in the East–West direction, and 21.4 km in the North–South direction. This DEM is shown in Figure 4 using a top view with isocontours representing the height of the topography every 0.2 km.

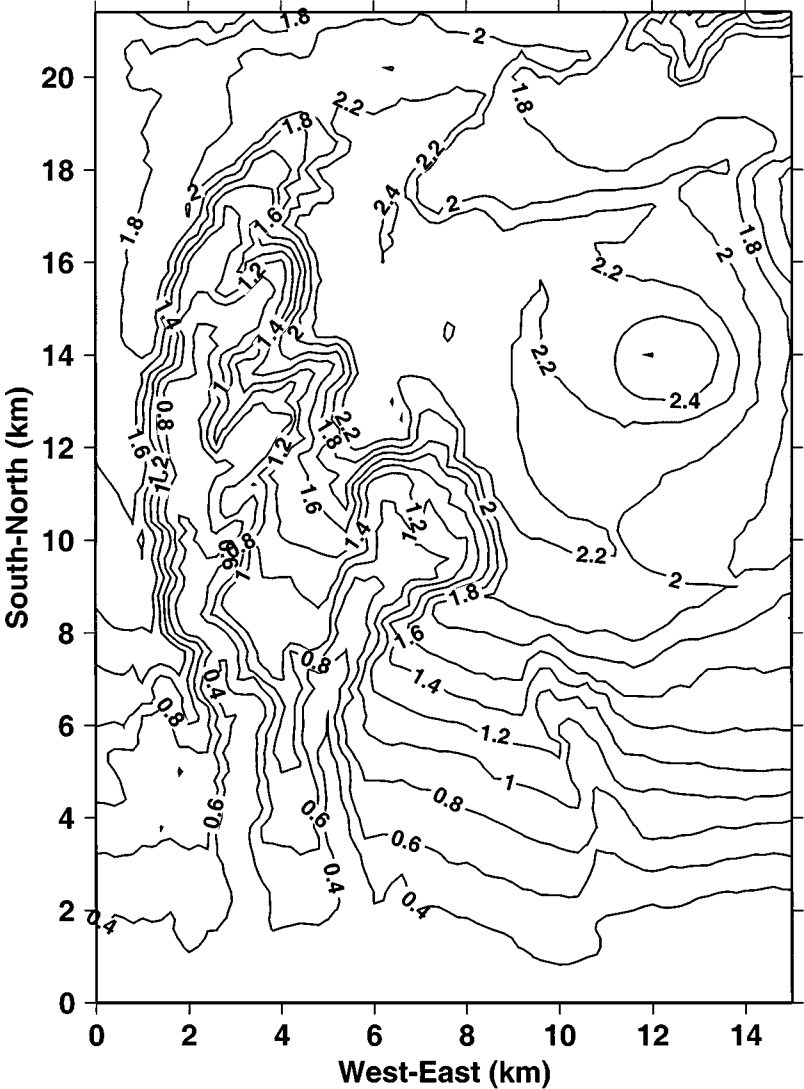


**Figure 4.** Isocontours of the DEM of the Piton de la Fournaise volcano. The DEM is given on a grid of  $76 \times 108$  points, with a uniform grid spacing of 200 m. The isocontours represent the height of the topography every 0.2 km. The height of the summit is 2.6 km. One can clearly observe the slopes of the two steep valleys.

In the preprocessing, we choose a regular distribution of the  $\{u_i\}$  in  $[\alpha, \beta] = [0, 1]$  in order to reduce the large variations in the data set. The approximants are subsequently obtained by discretizing the  $D^m$  spline in a finite-element space. In the case of the  $C^0$  approximant, we use  $30 \times 40$  rectangular  $C^0$  BFS finite elements, each having four degrees of freedom. In the case of the  $C^1$  approximant, we use  $15 \times 20$  rectangular  $C^1$ -BFS finite elements, each having sixteen degrees of freedom. In both cases, the smoothing parameter  $\varepsilon$  is taken to be  $10^{-6}$ .

In Figure 5, we show a three-dimensional representation of the  $C^1$  approximant after postprocessing, evaluated on an evenly spaced grid comprising  $200 \times 200$  points. The grid spacing in the East–West direction is therefore 107.54 m, and that in the North–South direction is 75.37 m. From the figure it is clear that the results do not exhibit strong oscillations, even though the use of such a dense grid for the evaluation of the approximant is expected to enhance the artefacts generated by the approximation method. To compare this approximant to the original data set more precisely, in Figure 6 we present a top view of the approximated values, with isocontours representing the height every 0.2 km, in addition to the same plot for the original data set, as in Figure 4. It is clear from these plots that the approximant is very close to the original data, with local variations smoothed as expected. One can notice that the approximant does not exhibit significant oscillations even in the difficult regions of the model, particularly the two valleys.

To demonstrate this more quantitatively, we evaluate the quadratic error for the two approximants

$$\text{Err}(\cup_i z_i) = \left( \frac{\sum_{i=1}^{8208} (\tilde{z}_i - z_i)^2}{\sum_{i=1}^{8208} z_i^2} \right)^{1/2} \quad (19)$$

where  $z_i$  represents the  $z$ -data value, and where  $\tilde{z}_i$  is the  $z$ -approximant value for the same  $(x_i, y_i) \in \Omega$ . In the case of the  $C^0$  approximant, we find that the error is  $4.96 \cdot 10^{-4}$ ; in the case of the  $C^1$  approximant it is  $4.01 \cdot 10^{-4}$ . Such values are considered very good in the context of surface approximation, and show the efficiency of the proposed approach for this case with rapidly varying data. In the entire data set, the maximum error measured is 5.5%, corresponding to an absolute error of 56 m. This maximum error occurs in a region located on the edge of the steep valleys, where the local variations are the strongest, as expected. More detailed studies of the approximation error, and evidence that the rate of convergence is higher in this method than in usual approaches with no preprocessing, such as splines under tension or thin plate splines, can be found in Gout (1997).

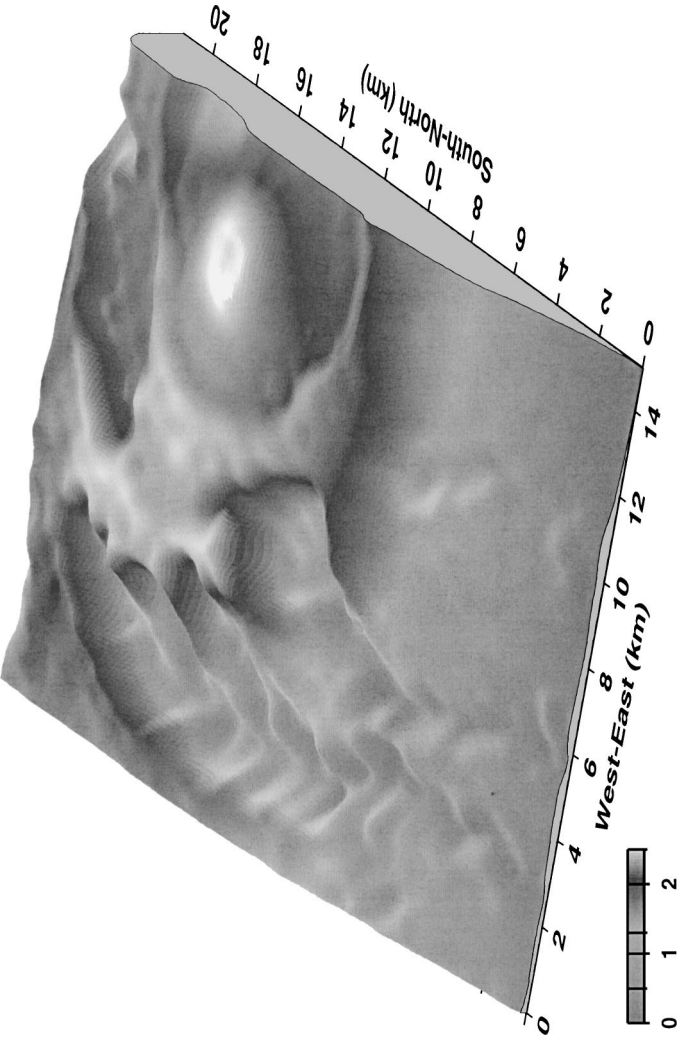


**Figure 5.** Three-dimensional view of the  $C^1$  approximant, after post-processing, obtained for the Piton de la Fournaise volcano from the Digital Elevation Model of Figure 4. The gray scale represents the height of the topography, from 0 to 2.6 km. The image has been generated with no vertical exaggeration. The approximant has been evaluated on an evenly spaced grid comprising  $200 \times 200$  points. No significant oscillations can be observed, even in the difficult regions of the model, which are mainly the two valleys, and also the caldera. In this example, we have discretized the spline using  $15 \times 20$  BFS finite elements, each having sixteen degrees of freedom.

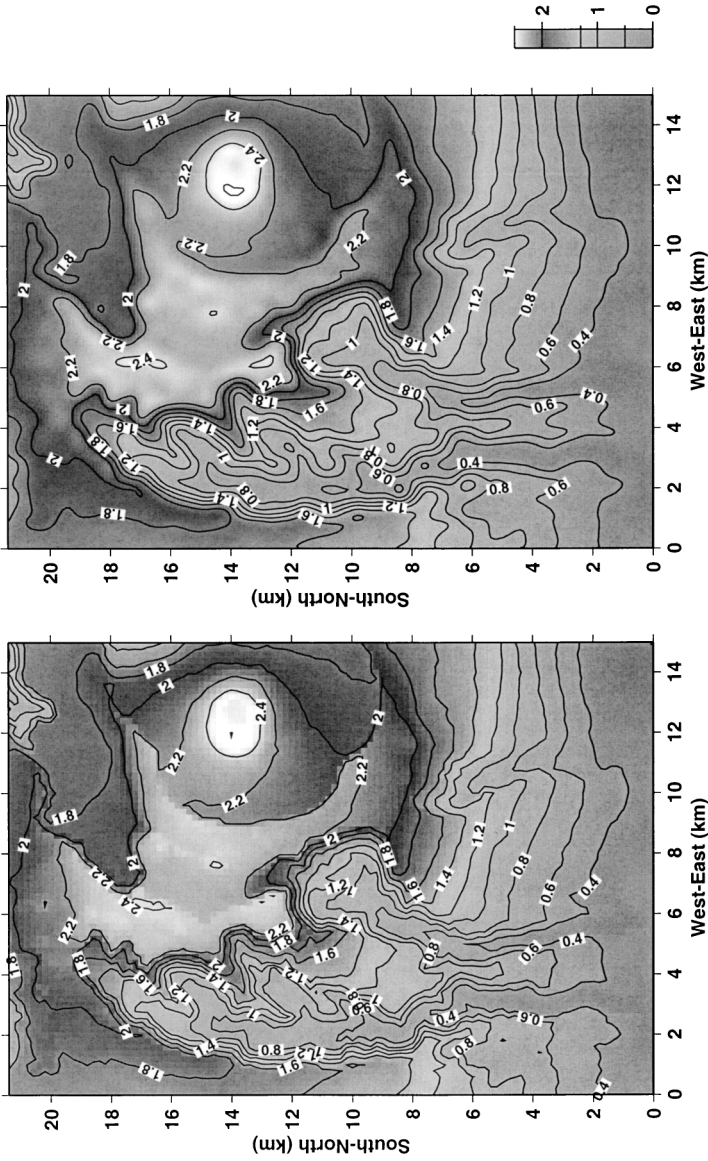


**Figure 6.** Comparison between the isocontours obtained from the original dataset of the DEM (left), as in Figure 4, and the isocontours of the  $C_1$  approximant after postprocessing (right), as in the three-dimensional view of Figure 5. The general agreement is excellent, and it is important to notice that no significant oscillations can be observed, even in the two steep valleys. Isocontours represent the height of the topography every 0.2 km. The gray scale also indicates the height of the topography, from 0 to 2.6 km.

## CONCLUSIONS

We have presented a new method to fit rapidly varying geophysical data. The capability to suppress, or at least significantly reduce, oscillations of the surface near steep gradients has been demonstrated. The scale transformation families introduced provide more control on the behavior of the approximant, without any particular a priori knowledge of the location of the large variations in the dataset. The regularity obtained, which can be  $C^0$ ,  $C^1$ , or higher, allows us to describe the topography of real geophysical surfaces accurately. We have shown the good properties of this approach by applying it to the real case of the Piton de la Fournaise volcano.

## ACKNOWLEDGMENTS

The authors would like to thank Ecole Annexe de Pau for making this collaboration possible. They would also like to thank Dominique Apprato for discussion, and Jeroen Tromp for support. The constructive comments of the two reviewers, J. J. Royer and S. Zoraster, significantly improved the manuscript. The image of the Piton de la Fournaise volcano is courtesy of Pete Mouginiis-Mark, University of Hawaii. This research has been funded in part by the David and Lucile Packard Foundation.

## REFERENCES

- Apprato, D., 1987, Approximation de surfaces paramétrées par éléments finis: unpubl. doctoral dissertation, Université de Pau et des Pays de l'Adour, Pau, France, Thèse d'Etat, 142 p.
- Arcangéli, R., 1986,  $D^m$ -splines sur un domaine borné de  $\mathbb{R}$ : Technical Report 1986/2, UA 1204 CNRS, Université de Pau et des Pays de l'Adour, Pau, France, 47 p.
- Arcangéli, R., 1989, Some applications of discrete  $D^m$ -splines, in Lyche, T., and Schumaker, L. L., eds., *Mathematical Methods in Computer Aided Geometric Design*: Academic Press, New York, p. 35–44.
- Bouchon, M., Schultz, C. A., and Töksoz, M. N., 1996, Effect of three-dimensional topography on seismic motion: *Jour. Geophys. Res.*, v. 101, p. 5835–5846.
- Bouhamidi, A., 1992, Interpolation et approximation par des fonctions splines radiales à plusieurs variables: unpubl. doctoral dissertation, Université de Nantes, Nantes, France, 190 p.
- Ciarlet, P. G., 1978, *The finite element method for elliptic problems*: North Holland, Amsterdam, 530 p.
- Foley, T. A., 1987, Weighted bicubic spline interpolation to rapidly varying data: *ACM Trans. Graphics*, v. 6, p. 1–18.
- Franke, R., 1985, Thin plate spline with tension: *Computer Aided Geometric Design*, v. 2, p. 87–95.
- Frankel, A., and Leith, W., 1992, Evaluation of topographic effects on  $P$  and  $S$  waves of explosions at the northern Novaya Zemlya test site using 3-D numerical simulations: *Geophys. Res. Lett.*, v. 19, p. 1887–1890.
- Gout, C., 1997, Etude de changements d'échelle en approximation—ajustement spline sur des morceaux de surfaces: unpubl. doctoral dissertation, Université de Pau et des Pays de l'Adour, Pau, France, 203 p.

- Gout, C., 1998, Approximation of curves and surfaces from rapidly varying data: Technical Report 1001, Center for Pure and Applied Mathematics, University of California at Berkeley, USA, 36 p.
- Gout, C., 1999, Approximation using scale transformations, *in* Chui, C. K., and Schumaker, L. L., eds., Approximation theory IX: Vanderbilt University Press, Nashville, v. 1, p. 151–158.
- Hsieh, H. C., and Chang, W. T., 1994, Virtual knot technique for curve fitting of rapidly varying data: Computer Aided Geometric Design, v. 11, p. 71–95.
- Ishihara, K., Iguchi, M., and Kamo, K., 1990, Numerical simulation of lava flows on some volcanoes in Japan, *in* Fink, J. H., ed., Lava flows and domes: Springer-Verlag, Berlin, p. 174–207.
- Issaks, E. H., and Srivastava, R. M., 1989, An introduction to applied geostatistics: Oxford University Press, Oxford, 560 p.
- Komatitsch, D., and Vilotte, J. P., 1998, The spectral element method: An efficient tool to simulate the seismic response of 2D and 3D geological structures: Bull. Seis. Soc. Am., v. 88, p. 368–392.
- Komatitsch, D., Vilotte, J. P., Vai, R., Castillo-Covarrubias, J. M., and Sánchez-Sesma, F. J., 1999, The spectral element method for elastic wave equations: Application to 2D and 3D seismic problems: Int. Jour. Numer. Meth. Engng., v. 45, p. 1139–1164.
- Mallet, J. L., 1992, Discrete smooth interpolation in geometric modeling: Computer-Aided Design, v. 24, p. 178–191.
- Mallet, J. L., 1997, Discrete modeling for natural objects: Math. Geology, v. 29, p. 199–219.
- Necas, J., 1967, Les méthodes directes en théorie des équations elliptiques: Masson, Paris, 351 p.
- Salkauskas, K., 1974,  $C^1$  splines for interpolation of rapidly varying data: Rocky Mountain Jour. Math., v. 14, p. 239–250.
- Torrens, J. J., 1991, Interpolación de superficies paramétricas con discontinuidades mediante elementos finitos, aplicaciones: unpubl. doctoral dissertation, Universidad de Zaragoza, Zaragoza, España, 186 p.